Electronic Supplementary Information (ESI)

Vertical *vs* Adiabatic Ionization Energies in Solution and Gas-Phase: Probing Ionization-Induced Reorganization in Conformationally-Mobile Bichromophoric Actuators using Photoelectron Spectroscopy, Electrochemistry and Theory

Maxim V. Ivanov, Denan Wang, Depeng Zhang, Rajendra Rathore[†] and Scott A. Reid*

[†]Deceased February 16, 2018

Corresponding author: scott.reid@marquette.edu

Department of Chemistry, Marquette University, Milwaukee, WI 53233

Table of Content

Synthesis

A series of similar veratrole- and acetal-based actuator molecules (**V2**, **V2**-locked, **Ac2**-C2H4, **Ac2**-CH2, Fig. S1) and model compound **V1** were synthesized from previously reported procedures[1-3] and were fully characterized by $^{1}H/^{13}C$ NMR spectroscopy.

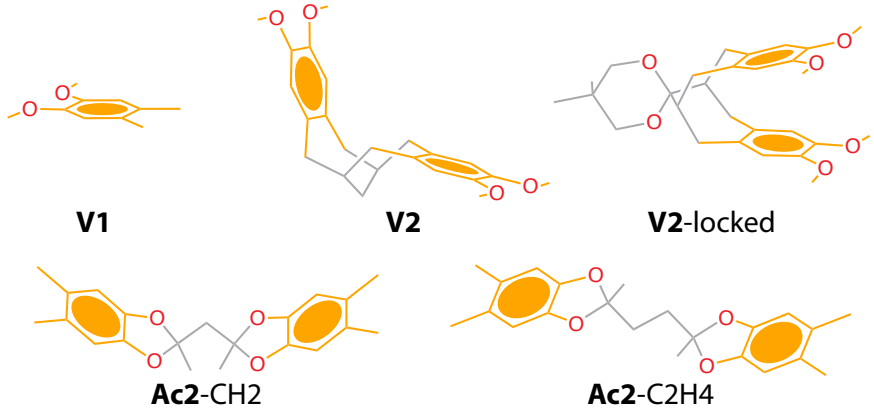

Fig. S1. Structures and naming scheme of the compounds studied in this work.

NMR spectroscopy

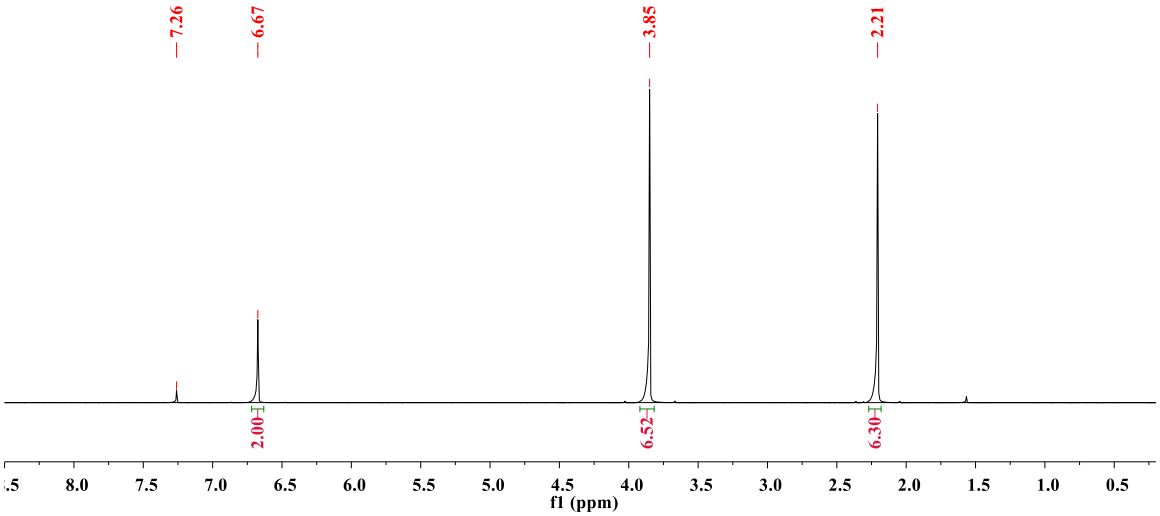

Fig. S2. ^{1}H-NMR spectrum of 1,2-dimethoxy-4,5-dimethylbenzene (**V1**)

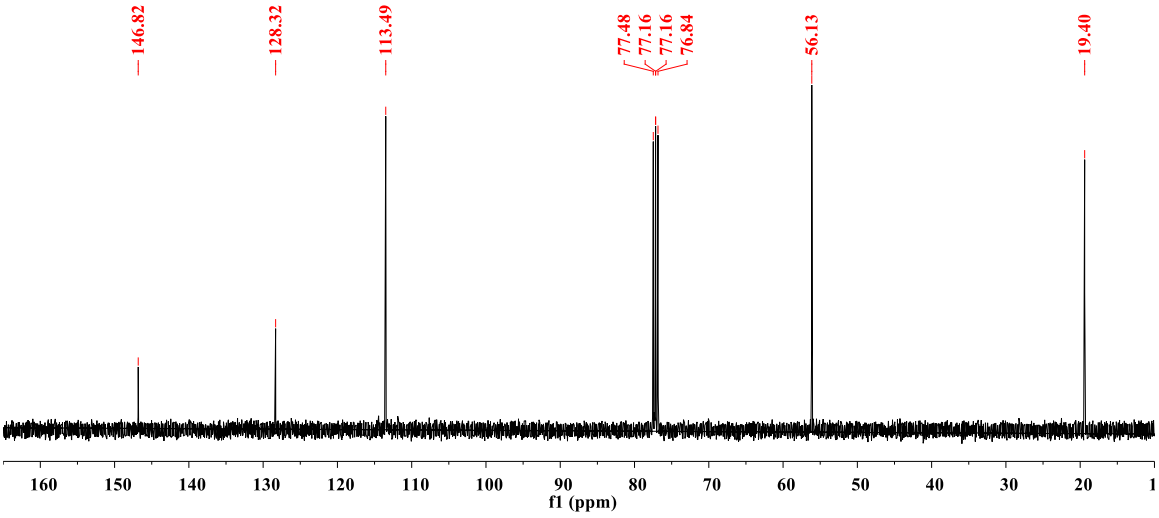

Fig. S3. ^{13}C-NMR spectrum of 1,2-dimethoxy-4,5-dimethylbenzene (**V1**)

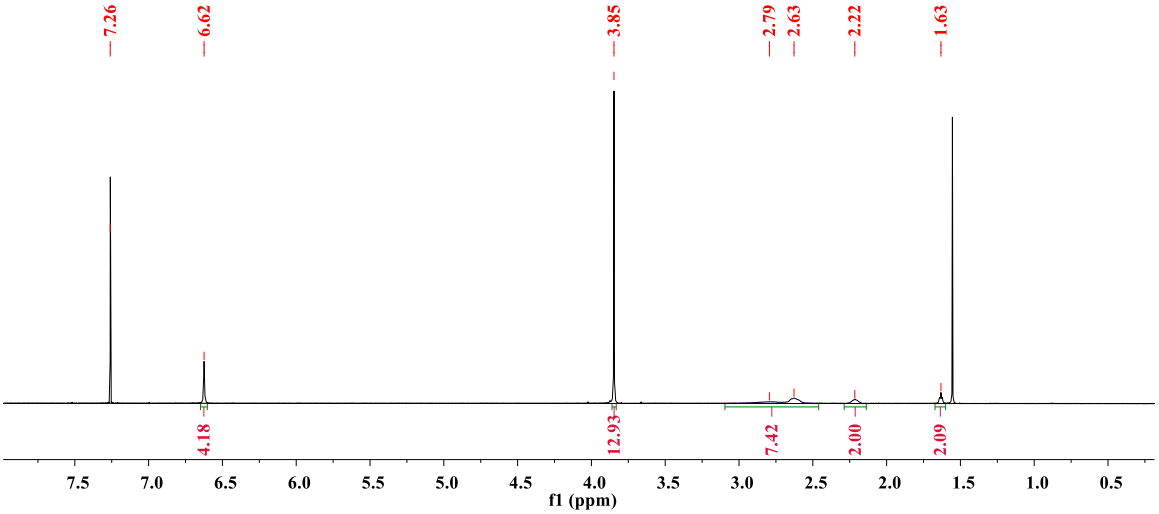

Fig. S4. ^{1}H-NMR spectrum of **V2**

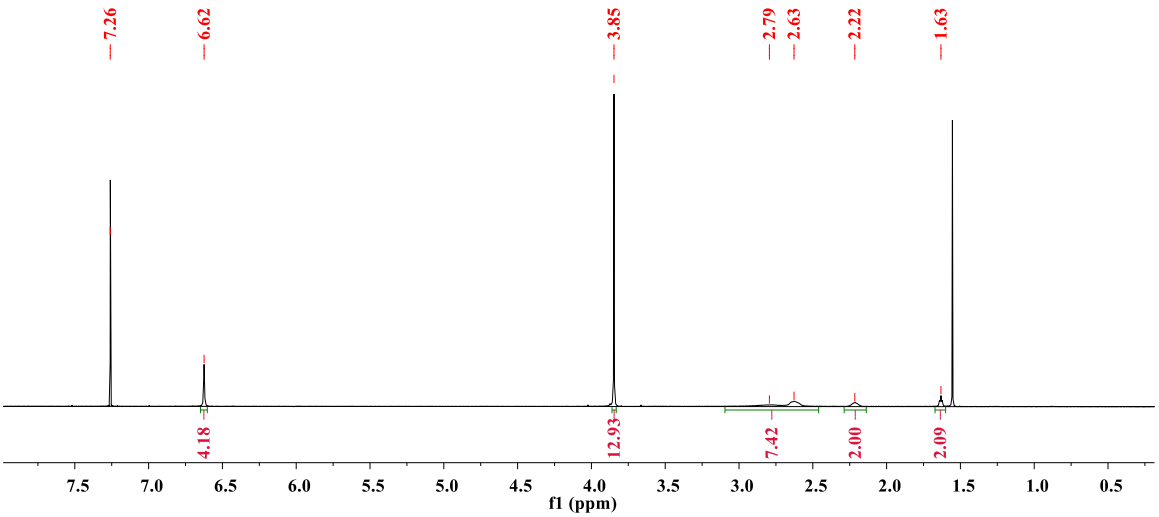

Fig. S5. ^{13}C-NMR spectrum of **V2**

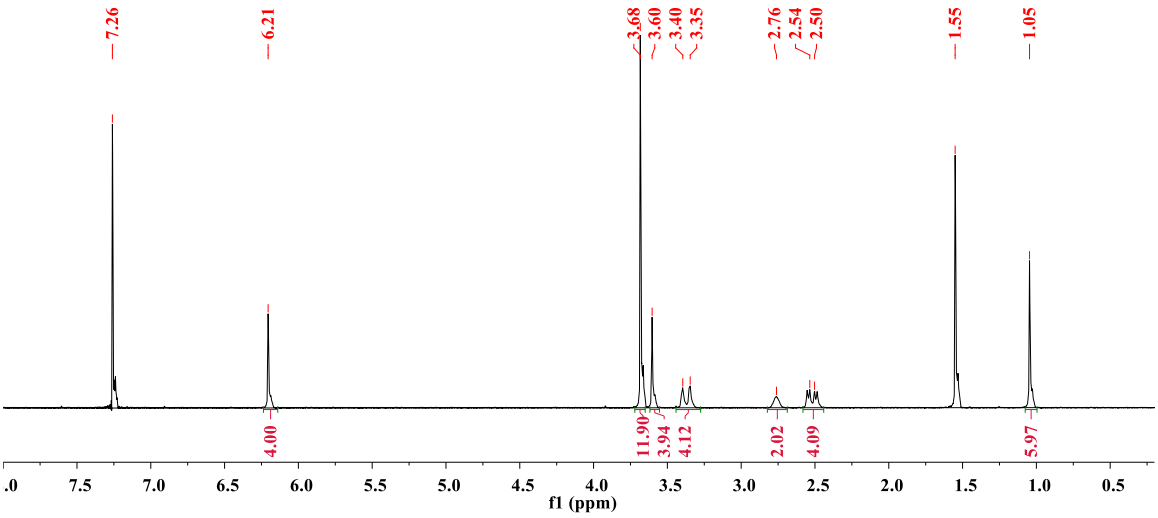

Fig. S6. [1]H-NMR spectrum of **V2**-locked

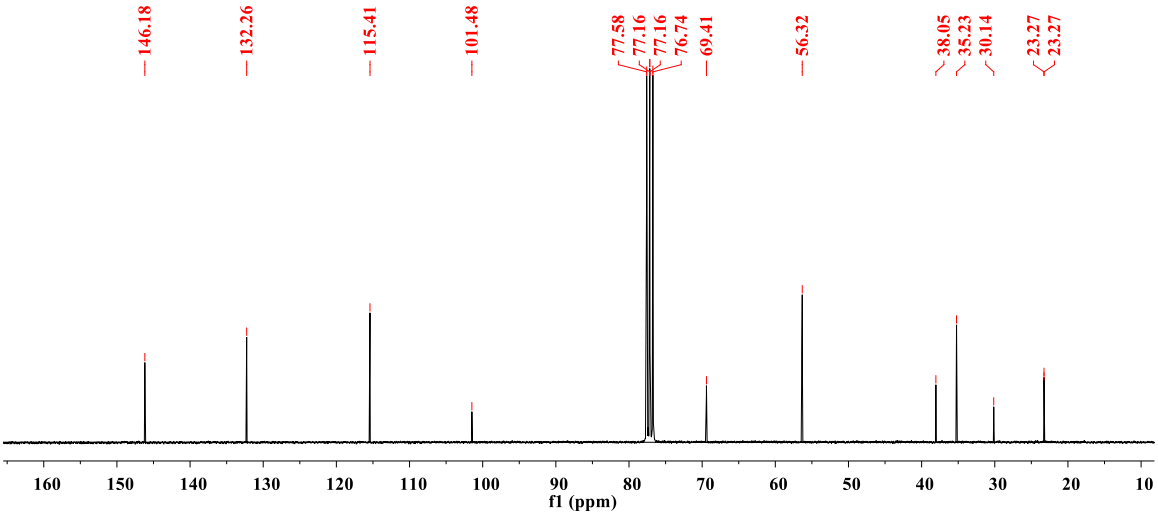

Fig. S7. [13]C-NMR spectrum of **V2**-locked

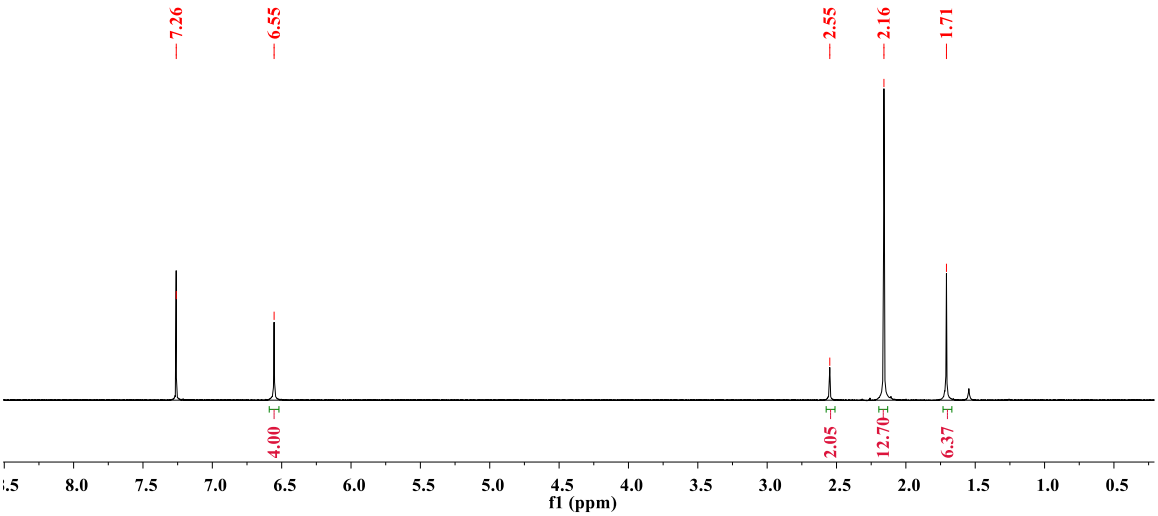

Fig. S8. [1]H-NMR spectrum of **Ac2**-CH2

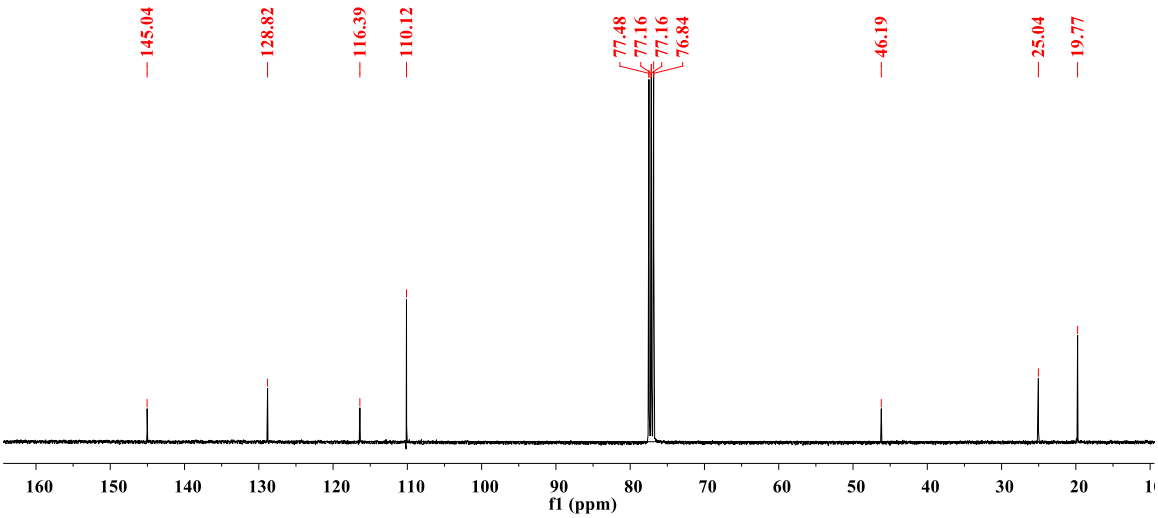

Fig. S9. ^{13}C-NMR spectrum of **Ac2**-CH2

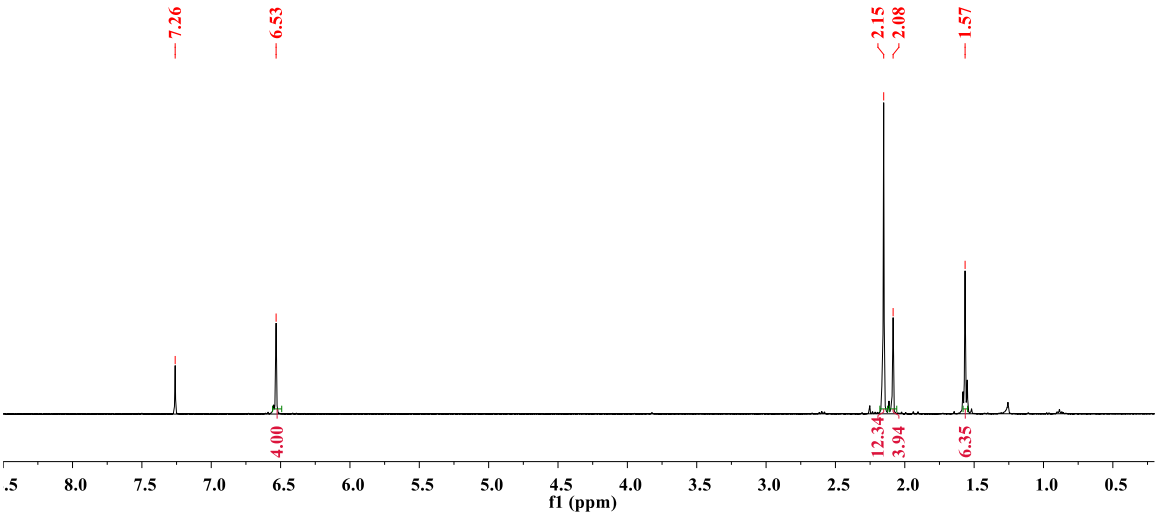

Fig. S10. ^{1}H-NMR spectrum of **Ac2**-C2H4

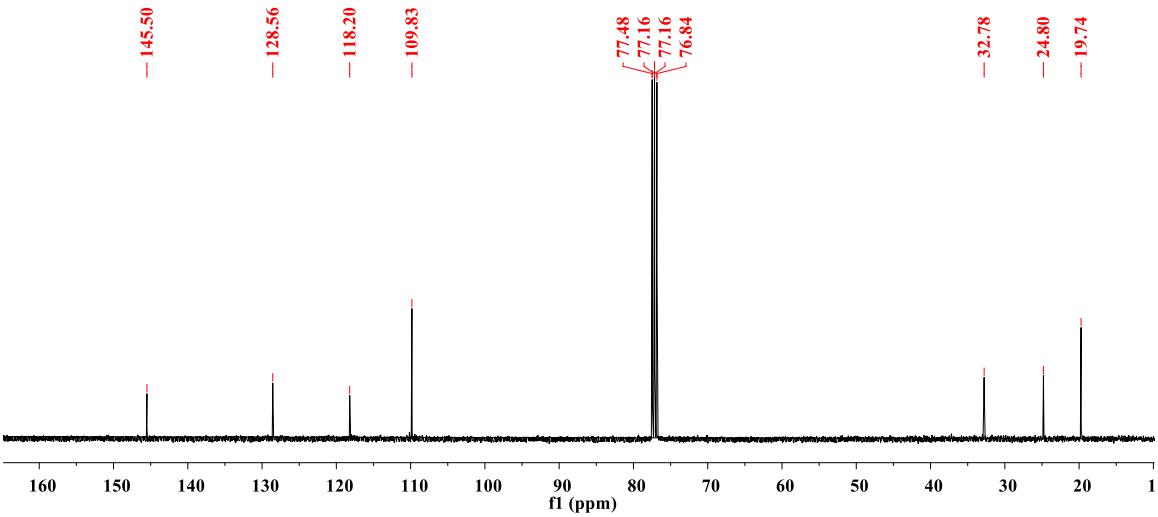

Fig. S11. ^{13}C-NMR spectrum of **Ac2**-C2H4

Electrochemistry

The cyclic voltammetry cell was of an air-tight design with high vacuum Teflon valves and Viton O-ring seals to allow an inert atmosphere to be maintained without contamination by grease. The working electrode consisted of an adjustable platinum disk embedded in a glass seal to allow periodic polishing (with a fine emery cloth) without changing the surface area (~1 mm^2) significantly. The reference SCE electrode (saturated calomel electrode) and its salt bridge were separated from the catholyte by a sintered glass frit. The counter electrode consisted of a platinum gauze that was separated from the working electrode by ~3 mm. The cyclic voltammetry measurements were carried out in a solution of 0.1 M supporting electrolyte (tetra-*n*-butylammonium hexafluorophosphate) and the substrate in dry CH_2Cl_2 under an argon atmosphere at 22 ºC. All the cyclic voltammograms were recorded at a sweep rate of 100 mV sec^{-1} and were IR compensated. The oxidation potentials (E_{ox}, calculated by taking the average of anodic and cathodic peaks) were referenced to ferrocene.

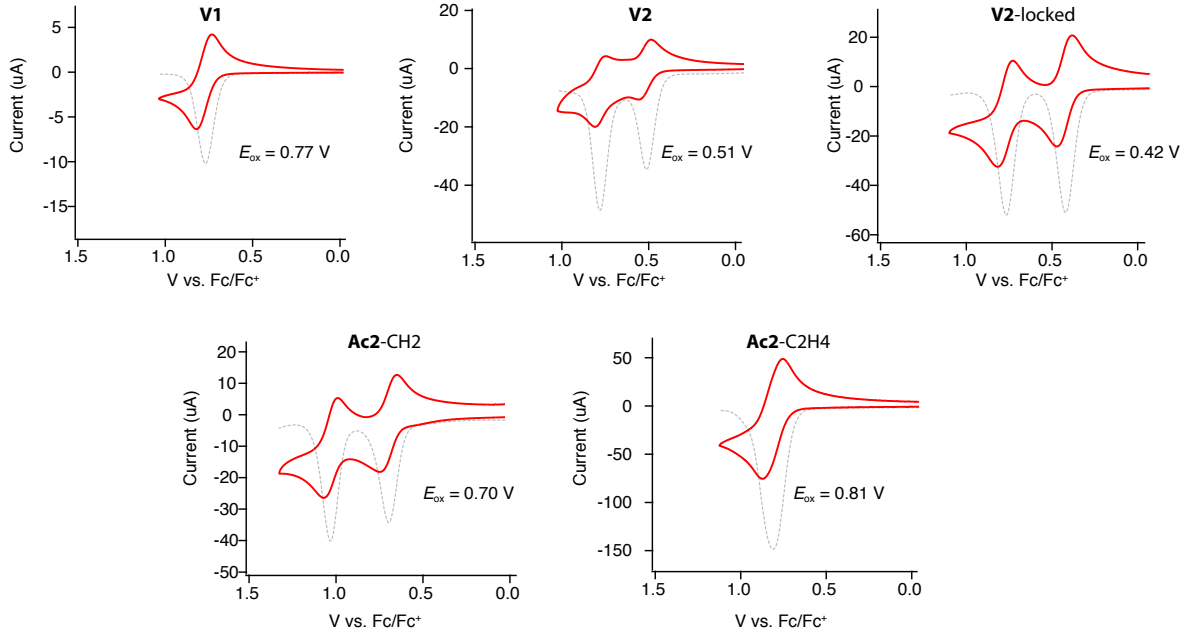

Fig. S12. Cyclic voltammograms of 2 mM **V1**, **V2**, **V2**-locked, **Ac2**-CH2 and **Ac2**-C2H4 in CH_2Cl_2 (0.1 M *n*-$Bu_4N^+PF_6^-$) at ν = 100 mV/s and 22 ˚C.

Density functional theory calculations

Computational details

All electronic structure calculations of were performed using density functional theory (DFT) in Gaussian 09 package.[4] In all DFT calculations, ultrafine Lebedev's grid was used with 99 radial shells per atom and 590 angular points in each shell. In cation radical calculations, wave function stability test[5] was performed to ensure absence of solutions with lower energy. The values of $<S^2>$ operator after spin annihilation were confirmed to be close to the expectation value of 0.75. Tight cutoffs on forces and atomic displacement were used to determine convergence in geometry optimization procedure. Harmonic vibrational frequency calculations were performed for the optimized structures to confirm absence of imaginary frequencies.

Accurate description of the electronic structure of the cation radicals of pi-conjugated and pi-stacked systems is challenging for DFT due to the self-interaction error that causes artificial hole delocalization and lowering of the ionization energies.[6-8] These artifacts can be minimized using a hybrid functional with a tuned portion of the exact Hartree-Fock (HF) exchange or range-separated density functional.[9,10] However, in many standard hybrid functionals amount of the Hartree-Fock exchange has not been parameterized for a correct description of the hole delocalization.[11,12] Recent studies of mixed-valence compounds[10,11,13] and poly-*p*-phenylene wires[14] have demonstrated that customization of a standard density functional by tuning the amount of the HF exchange to reproduce experimental data can provide a reliable description of the electronic structure of pi-conjugated cation radicals.

In our previous study[14] we have used a one-parameter B1LYP[15] functional where HF exchange was varied to accurately reproduce oxidation potentials and cation radical excitation energies of the poly-*p*-phenylenes with varied number of *p*-phenylenes. It was shown that 40% of the HF exchange provides a balanced description of the electronic structure of the poly-*p*-phenylene cation radicals, which is also similar to that shown by Kaupp and coworkers.[13] Usage of modified B1LYP-40/6-31G(d) functional performed exceptionally well in reproducing the experimental redox/optoelectronic properties of a variety of poly-*p*-phenylene-based wires[16-18] wires and other PAHs.[19,20] In order to account for dispersion interactions within B1LYP-40 functional we have utilized D3 version of Grimme's dispersion[21] parameters SR6 = 1.3780 and S8 = 1.2170 (analogous to those at CAM-B3LYP-D3). In recent studies we have shown[22,23] that such a modification provided an accurate description of the cation radical states of various pi-stacked bifluorene derivatives. In the same study it was shown that CAM-B3LYP-D3 provides a balanced description of the neutral, excited and cation radical state.

Accordingly, in this manuscript, we performed electronic structure calculations using CAM-B3LYP-D3 and B1LYP-40-D3 functionals with 6-31G(d) basis set. Energies of the optimized equilibrium structures in the gas phase were corrected for zero-point energy (ZPE) and basis set superposition error (BSSE) using counterpoise (CP) method. Solvent effects were included using the implicit integral equation formalism polarizable continuum model (IEF-PCM)[24-28] with dichloromethane as solvent. Free energies were computed within harmonic oscillator approximation for T = 298.15 K and P = 1 atm. Note that PCM calculations do not support counterpoise method and therefore to account for BSSE in calculations with solvent, the CP correction from gas phase calculations was applied.

Gas vs solution: role of environment on the relative energies (BSSE corrected)

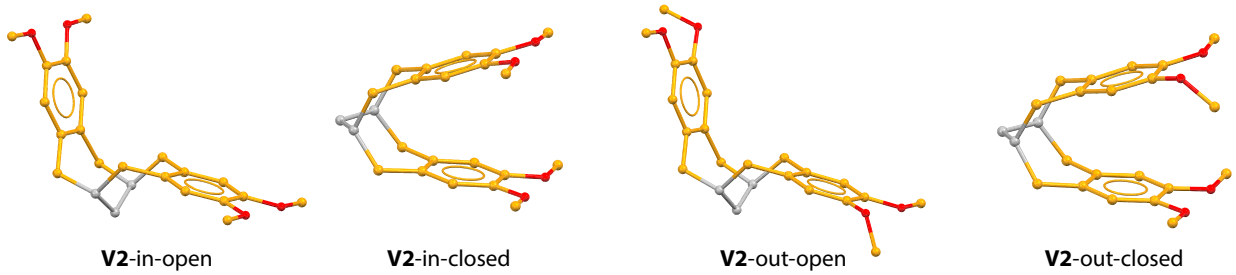

Fig. S13. Structures of **V2** conformers. Hydrogens are excluded for clarity.

Table S1. Relative energies of **V2** conformers in neutral (S_0) and cation radical (D_0) states in gas phase and vertical ionization energies (VIE) calculated using CAM-B3LYP-D3/6-31G(d) with counterpoise correction.

Conformers	$\Delta E[S_0]$, kcal/mol	$\Delta E[D_0]$, kcal/mol	VIE, eV
V2-in-closed	1.65	0.00	6.34
V2-in-open	0.90	8.12	6.70
V2-out-open	0.75	10.92	7.05
V2-out-closed	0.00	1.11	6.53

Table S2. Relative energies of **V2** conformers in neutral (S_0) and cation radical (D_0) states in CH_2Cl_2 calculated using CAM-B3LYP-D3/6-31G(d)+PCM with counterpoise correction.

Conformers	$\Delta E[S_0]$, kcal/mol	$\Delta E[D_0]$, kcal/mol
V2-in-closed	2.06	0.00
V2-in-open	0.00	3.36
V2-out-open	0.47	6.66
V2-out-closed	1.29	1.11

Table S3. Relative energies of **V2** conformers in neutral (S_0) and cation radical (D_0) states in gas phase and vertical ionization energies (VIE) calculated using B1LYP40-D3/6-31G(d) counterpoise BSSE correction.

Conformers	$\Delta E[S_0]$, kcal/mol	$\Delta E[D_0]$, kcal/mol	VIE, eV
V2-in-closed	1.66	0.00	6.15
V2-in-open	0.55	6.73	6.45
V2-out-open	0.00	n/a	6.78
V2-out-closed	0.16	1.23	6.34

Table S4. Relative energies of **V2** conformers in neutral (S_0) and cation radical (D_0) states in CH_2Cl_2 calculated using B1LYP40-D3/6-31G(d)+PCM with counterpoise correction.

Conformers	$\Delta E[S_0]$, kcal/mol	$\Delta E[D_0]$, kcal/mol
V2-in-closed	1.00	0.00
V2-in-open	0.00	3.92
V2-out-open	0.07	n/a
V2-out-closed	1.10	1.54

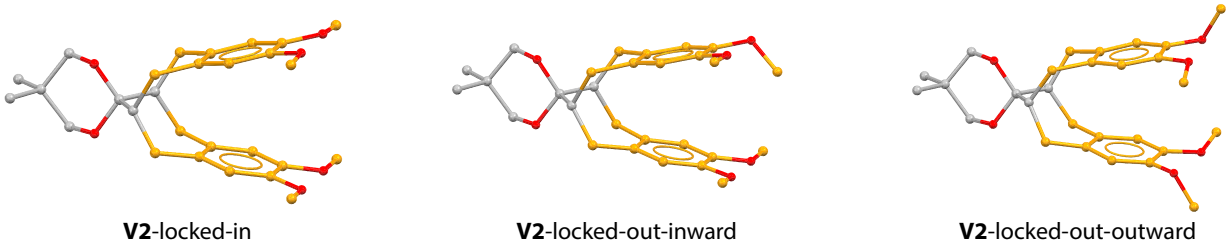

V2-locked-in **V2**-locked-out-inward **V2**-locked-out-outward

Fig. S14. Structures of **V2**-locked conformers. Hydrogens are excluded for clarity.

Table S5. Relative energies of **V2**-locked conformers in neutral (S_0) and cation radical (D_0) states in gas phase, vertical (VIE) and adiabatic (AIE) ionization energies calculated using CAM-B3LYP-D3/6-31G(d) with counterpoise correction.

Conformers	$\Delta E[S_0]$, kcal/mol	$\Delta E[D_0]$, kcal/mol	VIE, eV	AIE, eV
V2-locked-in	2.24	0.00	6.24	5.98
V2-locked-out-outward	0.00	1.84	6.53	6.15
V2-locked-out-inward	0.52	1.03	6.44	6.10

Table S6. Relative energies of **V2**-locked conformers in neutral (S_0) and cation radical (D_0) states in CH_2Cl_2 calculated using CAM-B3LYP-D3/6-31G(d)+PCM with counterpoise correction.

Conformers	$\Delta E[S_0]$, kcal/mol	$\Delta E[D_0]$, kcal/mol
V2-locked-in	0.83	0.00
V2-locked-out-outward	0.57	3.00
V2-locked-out-inward	0.00	1.65

Table S7. Relative energies of **V2**-locked conformers in neutral (S_0) and cation radical (D_0) states in gas phase, vertical (VIE) and adiabatic (AIE) ionization energies calculated using B1LYP40-D3/6-31G(d) with counterpoise correction.

Conformers	$\Delta E[S_0]$, kcal/mol	$\Delta E[D_0]$, kcal/mol	VIE, eV	AIE, eV
V2-locked-in	2.21	0.00	6.05	5.80
V2-locked-out-outward	0.00	2.09	6.33	5.99
V2-locked-out-inward	0.62	1.18	6.23	5.92

Table S8. Relative energies of **V2**-locked conformers in neutral (S_0) and cation radical (D_0) states in CH_2Cl_2 calculated using B1LYP40-D3/6-31G(d)+PCM with counterpoise correction.

Conformers	$\Delta E[S_0]$, kcal/mol	$\Delta E[D_0]$, kcal/mol
V2-locked-in	0.00	0.00
V2-locked-out-outward	0.95	4.41
V2-locked-out-inward	0.55	2.69

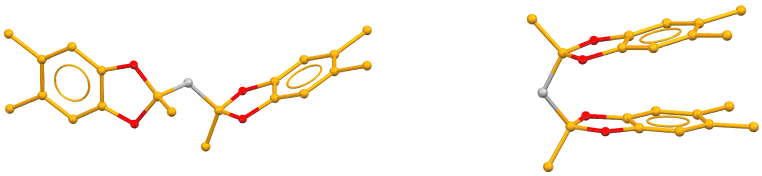

Ac2-CH2-open **Ac2**-CH2-closed

Fig. S15. Structures of **Ac2**-CH2 conformers. Hydrogens are excluded for clarity.

Table S9. Relative energies of **Ac2**-CH2 conformers in neutral (S_0) and cation radical (D_0) states in gas phase, vertical ionization energies (VIE) calculated using CAM-B3LYP-D3/6-31G(d) with counterpoise correction.

Conformers	$\Delta E[S_0]$, kcal/mol	$\Delta E[D_0]$, kcal/mol	VIE, eV
Ac2-CH2-closed	0.00	0.00	6.70
Ac2-CH2-open	0.30	9.62	7.02

Table S10. Relative energies of **Ac2**-CH2 conformers in neutral (S_0) and cation radical (D_0) states in CH_2Cl_2 calculated using CAM-B3LYP-D3/6-31G(d)+PCM with counterpoise correction.

Conformers	$\Delta E[S_0]$, kcal/mol	$\Delta E[D_0]$, kcal/mol
Ac2-CH2-closed	0.00	0.00
Ac2-CH2-open	0.02	8.44

Table S11. Relative energies of **Ac2**-CH2 conformers in neutral (S_0) and cation radical (D_0) states in gas phase, vertical ionization energies (VIE) calculated using B1LYP40-D3/6-31G(d) with counterpoise correction.

Conformers	$\Delta E[S_0]$, kcal/mol	$\Delta E[D_0]$, kcal/mol	VIE, eV
Ac2-CH2-closed	0.57	0.00	6.54
Ac2-CH2-open	0.00	6.85	6.75

Table S12. Relative energies of **Ac2**-CH2 conformers in neutral (S_0) and cation radical (D_0) states in CH_2Cl_2 calculated using B1LYP40-D3/6-31G(d)+PCM with counterpoise correction.

Conformers	$\Delta E[S_0]$, kcal/mol	$\Delta E[D_0]$, kcal/mol
Ac2-CH2-closed	0.61	0.00
Ac2-CH2-open	0.00	8.02

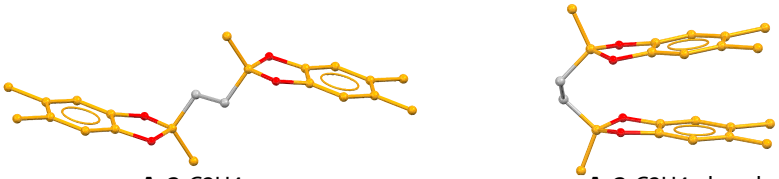

Fig. S16. Structures of **Ac2**-C2H4 conformers. Hydrogens are excluded for clarity.

Table S13. Relative energies of **Ac2**-C2H4 conformers in neutral (S_0) and cation radical (D_0) states in gas phase, vertical (VIE) and adiabatic (AIE) ionization energies calculated using CAM-B3LYP-D3/6-31G(d) with counterpoise correction.

Conformers	$\Delta E[S_0]$, kcal/mol	$\Delta E[D_0]$, kcal/mol	VIE, eV	AIE, eV
Ac2-C2H4-closed	1.05	0.00	6.89	6.63
Ac2-C2H4-open	0.00	3.74	7.02	6.84

Table S14. Relative energies of **Ac2**-C2H4 conformers in neutral (S_0) and cation radical (D_0) states in CH_2Cl_2 calculated using CAM-B3LYP-D3/6-31G(d)+PCM with counterpoise correction.

Conformers	$\Delta E[S_0]$, kcal/mol	$\Delta E[D_0]$, kcal/mol
Ac2-C2H4-closed	3.47	5.00
Ac2-C2H4-open	0.00	0.00

Table S15. Relative energies of **Ac2**-C2H4 conformers in neutral (S_0) and cation radical (D_0) states in gas phase, vertical (VIE) and adiabatic (AIE) ionization energies calculated using B1LYP40-D3/6-31G(d) with counterpoise correction.

Conformers	$\Delta E[S_0]$, kcal/mol	$\Delta E[D_0]$, kcal/mol	VIE, eV	AIE, eV
Ac2-C2H4-closed	2.00	0.37	6.66	6.51
Ac2-C2H4-open	0.00	0.00	6.72	6.59

Table S16. Relative energies of **Ac2**-C2H4 conformers in neutral (S_0) and cation radical (D_0) states in CH_2Cl_2 calculated using B1LYP40-D3/6-31G(d)+PCM with counterpoise correction.

Conformers	$\Delta E[S_0]$, kcal/mol	$\Delta E[D_0]$, kcal/mol
Ac2-C2H4-closed	0.00	5.52
Ac2-C2H4-open	0.44	0.00

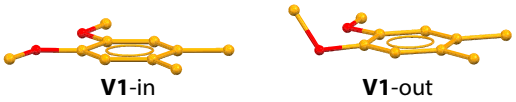

Fig. S17. Structures of **V1** conformers. Hydrogens are excluded for clarity.

Table S17. Relative energies of **V1** conformers in neutral (S_0) states in gas phase and CH_2Cl_2 calculated using B1LYP40-D3/6-31G(d) and CAM-B3LYP-D3/6-31G(d) without counterpoise correction. Note that in cation radical state of **V1** methoxy groups lie in the aromatic plane.

Conformers	CAM-B3LYP-D3/6-31G(d)			B1LYP40-D3/6-31G(d)		
	$\Delta E[S_0]$ gas	VIE, eV	$\Delta E[S_0]$ CH_2Cl_2	$\Delta E[S_0]$ gas	VIE, eV	$\Delta E[S_0]$ CH_2Cl_2
V1-in	0.00	7.09	0.00	0.19	6.95	0.00
V1-out	0.01	7.45	0.39	0.00	7.30	0.18

Quantifying BSSE: neutral vs cation radical state

Table S18. Relative energies (in kcal/mol) of various compounds in neutral (S_0) and cation radical (D_0) states calculated using CAM-B3LYP-D3/6-31G(d) with and without counterpoise correction in gas phase. BSSE (in kcal/mol) is calculated as the difference between total (ZPE-corrected) energies of the equilibrium structures calculated with and without counterpoise correction.

Compounds	With counterpoise correction		No counterpoise correction		BSSE	
	$\Delta E[S_0]$	$\Delta E[D_0]$	$\Delta E[S_0]$	$\Delta E[D_0]$	S_0	D_0
V2-in-closed	1.65	0.00	1.64	0.00	19.73	17.37
V2-in-open	0.90	8.12	3.64	10.52	16.97	14.97
V2-out-open	0.75	10.92	3.79	13.42	16.68	14.88
V2-out-closed	0.00	1.11	0.00	0.41	19.72	18.07
V2-locked-in	2.24	0.00	1.98	0.00	22.27	19.87
V2-locked-out-outward	0.00	1.84	0.00	1.00	22.00	20.72
V2-locked-out-inward	0.52	1.03	0.17	0.25	22.35	20.66
Ac2-CH2-closed	0.00	0.00	0.00	0.00	11.16	10.58
Ac2-CH2-open	0.30	9.62	1.42	11.30	10.04	8.90
Ac2-C2H4-closed	1.05	0.00	1.59	0.00	8.02	11.84
Ac2-C2H4-open	0.00	3.74	0.00	7.92	8.57	7.67

Table S19. Relative energies (in kcal/mol) of various compounds in neutral (S_0) and cation radical (D_0) states calculated using B1LYP40-D3/6-31G(d) with and without counterpoise correction in gas phase. BSSE (in kcal/mol) is calculated as the difference between total (ZPE-corrected) energies of the equilibrium structures calculated with and without counterpoise correction.

Compounds	With counterpoise correction		No counterpoise correction		BSSE	
	$\Delta E[S_0]$	$\Delta E[D_0]$	$\Delta E[S_0]$	$\Delta E[D_0]$	S_0	D_0
V2-in-closed	1.66	0.00	2.38	0.00	17.16	15.77
V2-in-open	0.55	6.73	2.47	8.60	15.95	13.91
V2-out-open	0.00	n/a	2.20	12.11	15.68	n/a
V2-out-closed	0.16	1.23	0.00	0.62	18.04	16.38
V2-locked-in	2.21	0.00	2.96	0.00	19.47	17.92
V2-locked-out-outward	0.00	2.09	0.00	1.37	20.23	18.64
V2-locked-out-inward	0.62	1.18	0.53	0.50	20.32	18.61
Ac2-CH2-closed	0.57	0.00	0.00	0.00	9.84	9.54
Ac2-CH2-open	0.00	6.85	0.38	8.38	8.89	8.01
Ac2-C2H4-closed	2.00	0.37	3.50	0.00	6.26	11.05
Ac2-C2H4-open	0.00	0.00	0.00	3.59	7.76	7.09

Quantifying BSSE: role of fragments

In intermolecular complexes the BSSE often arises due to the lack of flexibility of the basis set of each monomer leading to the wrong binding energies or even to incorrect geometries and vibrational frequencies.[29-31] When calculating the binding energy of a dimer using the CP method, the energy of each monomer (or fragment) is calculated using the basis set of both monomers in a dimer. While in the case of intermolecular complexes the definition of a fragment is obvious, in the case of covalently linked bichromophores, a choice of atomic content and electronic structure (i.e., charge and multiplicity) of each fragment becomes ambiguous. In this work, all bichromophores were separated into three fragments, i.e., two aromatic moieties and the linker, using two approaches (A and B, Fig. S18). Unfortunately, approach B had difficulties with geometry optimizations at the cation radical state and therefore approach A was employed throughout the study. Below we compare two approaches in the calculations of the energies of neutral bichromophores.

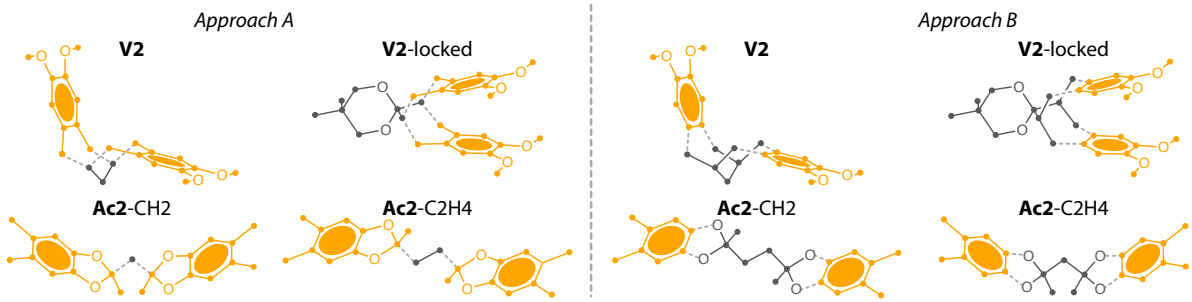

Fig. S18. Illustration of two approaches used to fragmentize bichromophoric molecules

Table S20. Relative energies and BSSE error of various compounds in neutral (S_0) state states calculated using CAM-B3LYP-D3/6-31G(d) with the counterpoise corrections in gas phase. Fragmentation of each bichromophore in the counterpoise method was employed via approach A and B as shown in Fig. S18. All values are in kcal/mol.

Compounds	Approach A		Approach B	
	$\Delta E[S_0]$	BSSE	$\Delta E[S_0]$	BSSE
V2-in-closed	1.65	19.73	1.55	20.03
V2-in-open	0.90	16.97	0.56	17.04
V2-out-open	0.75	16.68	0.43	16.77
V2-out-closed	0.00	19.72	0.00	20.13
V2-locked-in	2.24	22.27	2.06	20.07
V2-locked-out-outward	0.00	22.00	0.00	19.99
V2-locked-out-inward	0.52	22.35	0.44	20.26
Ac2-CH2-closed	0.00	11.16	1.23	17.18
Ac2-CH2-open	0.30	10.04	0.00	14.53
Ac2-C2H4-closed	1.05	8.02	0.00	11.83
Ac2-C2H4-open	0.00	8.57	1.13	14.55

Table S21. Relative energies and BSSE error of various compounds in neutral (S_0) state states calculated using B1LYP40-D3/6-31G(d) with the counterpoise corrections in gas phase. Fragmentation of each bichromophore in the counterpoise method was employed via approach A and B as shown in Fig. S18. All values are in kcal/mol.

Compounds	Approach A		Approach B	
	$\Delta E[S_0]$	BSSE	$\Delta E[S_0]$	BSSE
V2-in-closed	1.66	1.89	17.16	17.59
V2-in-open	0.55	0.53	15.95	16.13
V2-out-open	0.00	0.00	15.68	15.88
V2-out-closed	0.16	0.48	18.04	18.56
V2-locked-in	2.21	2.02	19.47	17.72
V2-locked-out-outward	0.00	0.00	20.23	18.67
V2-locked-out-inward	0.62	0.52	20.32	18.65
Ac2-CH2-closed	0.57	1.94	9.84	15.57
Ac2-CH2-open	0.00	0.00	8.89	13.25
Ac2-C2H4-closed	2.00	0.00	6.26	9.66
Ac2-C2H4-open	0.00	0.10	7.76	13.26

Table S22. Comparison of the experimental vertical (VIE) and adiabatic (AIE) energies, oxidation potentials (E_{ox}) with the corresponding computed values using two functionals.

Compounds	Experiment			CAM-B3LYP-D3/6-31G(d)			B1LYP40-D3/6-31G(d)		
	VIE	AIE	E_{ox}	VIE	AIE	G_{ox}	VIE	AIE	G_{ox}
V1	7.45	7.16	0.77	7.05	6.71	5.33	6.95	6.67	5.19
V2	7.25	6.71	0.51	6.7	6.12	5.05	6.45	5.96	4.88
V2-locked	7.06	6.67	0.42	6.44	6.05	4.97	6.23	5.87	4.77
Ac2-CH2	7.47	6.99	0.70	7.02	6.43	5.27	6.75	6.32	5.16
Ac2-C2H4	7.45	7.09	0.81	7.02	6.68	5.42	6.72	6.60	5.31

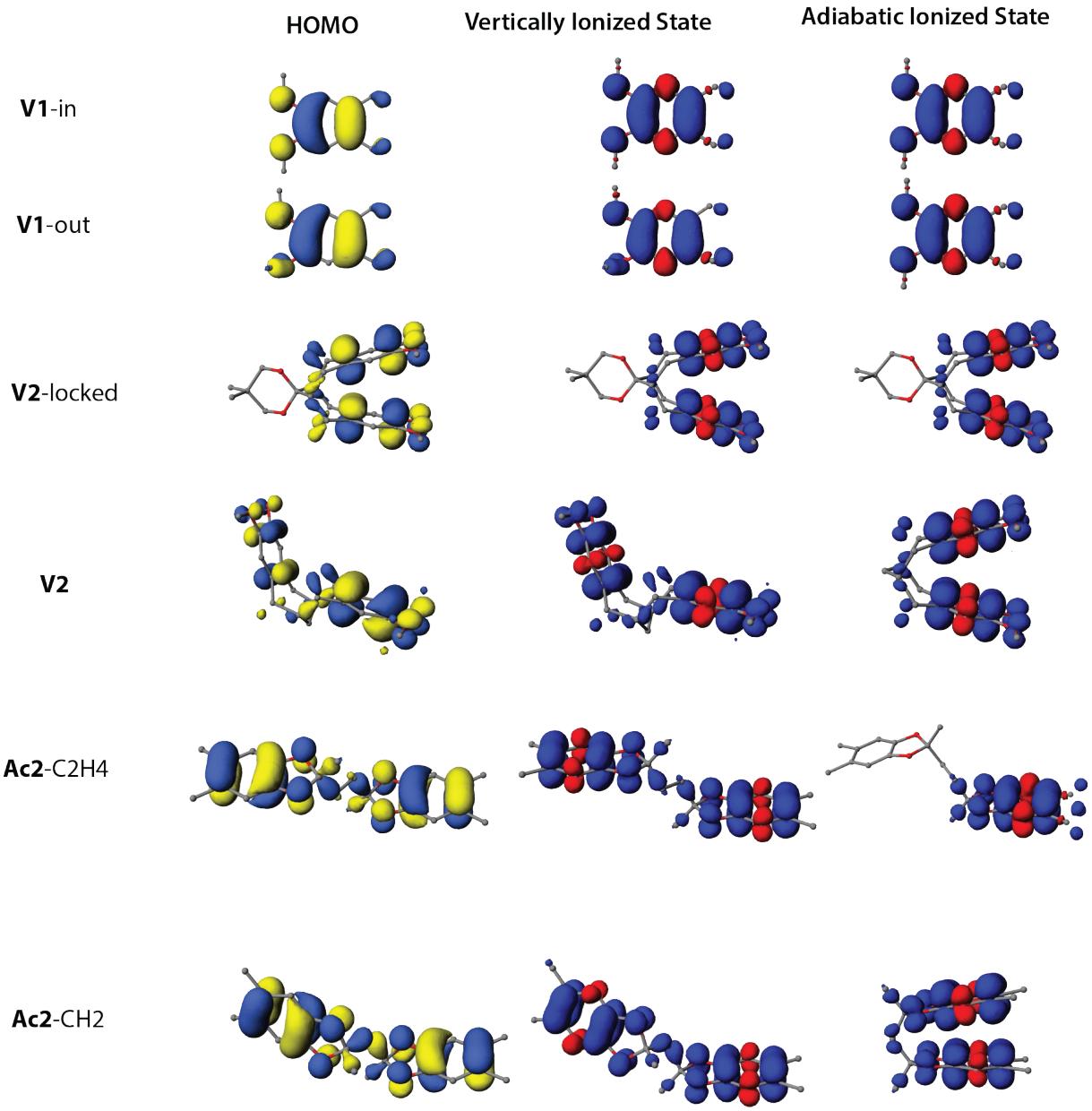

Fig. S19. HOMO plots of neutral compounds, spin-density plots at vertically ionized (gas-phase) and adiabatically ionized (solution) states calculated using CAM-B3LYP-D3/6-31G(d).

References

1. R. Shukla, K. Thakur, V. J. Chebny, S. A. Reid, and R. Rathore, *J. Phys. Chem. B.* 2010, **114**, 14592-14595.
2. V. J. Chebny, R. Shukla, S. V. Lindeman, and R. Rathore, *Org. Lett.* 2009, **11**, 1939-1942.
3. R. Rathore, V. J. Chebny, E. J. Kopatz, and I. A. Guzei, *Angew. Chem. Int. Ed.* 2005, **44**, 2771-2774.
4. Frisch, M. J.; Trucks, G. W.; Schlegel, H. B.; Scuseria, G. E.; Robb, M. A.; Cheeseman, J. R.; Scalmani, G.; Barone, V.; Mennucci, B.; Petersson, et. al. Gaussian, Inc., Wallingford CT, 2009
5. R. Bauernschmitt and R. Ahlrichs, *J. Chem. Phys.* 1996, **104**, 9047-9052.
6. D. S. Ranasinghe, J. T. Margraf, Y. Jin, and R. J. Bartlett, *J. Chem. Phys.* 2017, **146**, 034102.
7. M. Lundberg and P. E. M. Siegbahn, *J. Chem. Phys.* 2005, **122**, 224103.
8. Y. Zhang and W. Yang, *J. Chem. Phys.* 1998, **109**, 2604-2608.
9. M. Félix and A. A. Voityuk, *Int. J. Quantum. Chem.* 2011, **111**, 191-201.
10. M. Kaupp, M. Renz, M. Parthey, M. Stolte, F. Würthner, and C. Lambert, *Phys. Chem. Chem. Phys.* 2011, **13**, 16973-16986.
11. M. Renz, M. Kess, M. Diedenhofen, A. Klamt, and M. Kaupp, *J. Chem. Theory. Comput.* 2012, **8**, 4189-4203.
12. J. Yang, W. Zhang, Y. Si, and Y. Zhao, *J. Phys. Chem. B.* 2012, **116**, 14126-14135.
13. M. Renz, K. Theilacker, C. Lambert, and M. Kaupp, *J. Am. Chem. Soc.* 2009, **131**, 16292-16302.
14. M. R. Talipov, A. Boddeda, Q. K. Timerghazin, and R. Rathore, *J. Phys. Chem. C.* 2014, **118**, 21400-21408.
15. C. Adamo and V. Barone, *Chem. Phys. Lett.* 1997, **274**, 242-250.
16. D. Wang, M. R. Talipov, M. V. Ivanov, and R. Rathore, *J. Am. Chem. Soc.* 2016, **138**, 16337-16344.
17. M. V. Ivanov, V. J. Chebny, M. R. Talipov, and R. Rathore, *J. Am. Chem. Soc.* 2017, **139**, 4334-4337.
18. M. V. Ivanov, M. R. Talipov, A. Boddeda, S. H. Abdelwahed, and R. Rathore, *J. Phys. Chem. C.* 2017, **121**, 1552-1561.
19. M. V. Ivanov, K. Thakur, A. Boddeda, D. Wang, and R. Rathore, *J. Phys. Chem. C.* 2017, **121**, 9202-9208.
20. M. V. Ivanov, K. Thakur, A. Bhatnagar, and R. Rathore, *Chem. Commun. (Camb).* 2017, **53**, 2748-2751.
21. S. Grimme, A. Hansen, J. G. Brandenburg, and C. Bannwarth, *Chem. Rev.* 2016, **116**, 5105-5154.
22. B. Uhler, M. V. Ivanov, D. Kokkin, N. Reilly, R. Rathore, and S. A. Reid, *J. Phys. Chem. C.* 2017, **121**, 15580-15588.
23. D. Kokkin, M. V. Ivanov, J. Loman, J. -Z. Cai, R. Rathore, and S. A. Reid, *J. Phys. Chem. Lett.* 2018, 2058-2061.
24. J. Tomasi, B. Mennucci, and R. Cammi, *Chem. Rev.* 2005, **105**, 2999-3094.
25. S. Miertus, E. Scrocco, and J. Tomasi, *Chem. Phys.* 1981, **55**, 117-129.

26. M. Cossi, V. Barone, B. Mennucci, and J. Tomasi, *Chem. Phys. Lett.* 1998, **286**, 253-260.
27. E. Cances, B. Mennucci, and J. Tomasi, *J. Chem. Phys.* 1997, **107**, 3032-3041.
28. R. F. Ribeiro, A. V. Marenich, C. J. Cramer, and D. G. Truhlar, *J. Phys. Chem. B.* 2011, **115**, 14556-14562.
29. D. Moran, A. C. Simmonett, F. E. Leach, W. D. Allen, P. V. R. Schleyer, and H. F. Schaefer, *J. Am. Chem. Soc.* 2006, **128**, 9342-9343.
30. J. M. Martin, P. R. Taylor, and T. J. Lee, *Chem. Phys. Lett.* 1997, **275**, 414 - 422.
31. D. Asturiol, M. Duran, and P. Salvador, *J. Chem. Phys.* 2008, **128**, 144108.